ARTICLE

Mechanical and Water-Holding Properties and Microstructures of Soy Protein Isolate Emulsion Gels Induced by CaCl$_2$, Glucono-δ-lactone (GDL), and Transglutaminase: Influence of Thermal Treatments before and/or after Emulsification

Chuan-He Tang,*[,†,‡] Ling Chen,[†] and Edward Allen Foegeding[§]

[†]Department of Food Science and Technology and [‡]State Key Laboratory of Pulp and Paper Engineering, South China University of Technology, Guangzhou 510640, People's Republic of China

[§]Department of Food, Bioprocessing and Nutrition Sciences, North Carolina State University, Box 7624, Raleigh, North Carolina 27695-7624, United States

ABSTRACT: The mechanical properties, water-holding capacities (WHC), and microstructures of emulsion gels, induced by glucono-δ-lactone (GDL), CaCl$_2$, and microbial transglutaminase (MTGase) from unheated and heated soy protein isolate (SPI)-stabilized emulsions (at protein concentration 5%, w/v; oil volume fraction, 20%, w/v), were investigated and compared. The influence of thermal pretreatments (at 90 °C for 5 min) before and/or after emulsification was evaluated. Considerable differences in mechanical, water-holding, and microstructural properties were observed among various emulsion gels. The thermal pretreatment after emulsification increased the strength of the emulsion gels induced by GDL and CaCl$_2$, whereas in the case of MTGase, thermal pretreatments before and/or after emulsification on the contrary greatly inhibited gel network formation. The application of the enzyme coagulant exhibited much higher potential to form SPI-stabilized emulsion gels with higher mechanical strength than that of the other two coagulants. The WHC of the emulsion gels seemed to be not directly related to their gel network strength. Confocal laser scanning microscope analyses indicated that the network microstructure of the formed emulsion gels, mainly composed of aggregated protein-stabilized oil droplets and protein aggregate clumps, varied with the type of applied coagulants and emulsions. The differences in microstructure were basically consistent with the differences in mechanical properties of the gels. These results could provide valuable information for the formation of cold-set soy protein-stabilized emulsion gels.

KEYWORDS: soy protein emulsion, emulsion gel, microstructure, heat pretreatment, cold-set

■ INTRODUCTION

Protein-stabilized emulsion gel has attracted growing attention from the food industry, because many important food systems, such as cheese and processed meats, are emulsion gels. Additionally, it exhibits good potential to be applied as controlled-release carriers, especially for lipid-soluble bioactive ingredients. The protein-stabilized emulsion gels can be formed by means of heat treatment, acidification with glucono-δ-lactone (GDL), the addition of divalent salts (e.g., CaCl$_2$), and even enzymatic cross-linking with transgluatminase.[1−4] Gels formed by thermal and nonthermal treatments are generally called "heat-set" and "cold-set", respectively. The heat-set emulsion gels are clearly not suitable as carriers for heat-labile bioactives. The use of cold-set emulsion gels for carriers of heat-labile bioactive compounds is a relatively new area. For example, Liang et al.[4] successfully developed a cold-set β-lactoglobulin (the main globular protein in whey proteins) emulsion gel induced by Ca^{2+} that acted as the carrier of a fat-soluble compound (α-tocopherol), and it was indicated that the stability of released α-tocopherol was greatly improved during an in vitro digestion model.

To date, investigations of the preparation and properties of protein-stabilized emulsion gels, especially heat-set gels, have been widely performed using milk proteins and whey proteins in particular.[1−3,5−14] In many of these cases, for example, in heat- or acid-set gel systems, the protein-stabilized oil droplets have been generally considered as a kind of "active filler" strengthening the gel matrix, and as a consequence, the increase in oil fraction would result in remarkable increases in magnitude of mechanical strength of the gels. In the case of cold-set whey protein emulsion gels using GDL and CaCl$_2$ as the coagulants, heat treatment of the protein dispersions before emulsification is critically required to ensure formation of soluble aggregates.[3,5,12] By contrast, little evidence exists in the literature on investigations of the emulsion gels from other proteins (e.g., soy proteins). With an increase in the applications of soy protein products in food formulations, due to their good functional and health effects, there is a necessity to investigate the preparation and properties of soy protein-stabilized emulsion gels.

Kim and others[15] studied the rheological properties of heat-set soy protein gels containing oil droplets at various volume fractions ($\varnothing$ = 0−0.3) using small and large deformation techniques, in the absence and presence of 0.2 M NaCl. They found that the mechanical moduli of the gels formed upon heating and cooling increased with increasing $\varnothing$, and the moduli

were much higher if NaCl was added. In other words, the oil droplets were a kind of active filler under those conditions. Lee and others[16] investigated and compared the rheological and microstructure of sodium caseinate- and soy protein isolate (SPI)-stabilized emulsion gels induced by microbial transglutamiase (MTGase) and found that these two emulsion gels exhibited different microstructures and physical properties, but the formation of both emulsion gels could improve the texture of the emulsions and the stability and controlled-release of aroma compounds. In a more recent work, it was indicated that the properties of SPI emulsion gels induced by GDL acidification varied with the type of applied oil phases, and the emulsions from solid fat had higher gelation ability compared with liquid oil.[17] However, information addressing those cold-set soy protein-stabilized emulsion gels induced by various coagulants (e.g., GDL, CaCl$_2$ and transglutaminase) is limited, such as the gelation mechanism and the properties of formed gels. Furthermore, the influence of thermal treatment of the emulsions before or after the emulsification on the properties of emulsion gels is also not addressed in the literature, although it has been confirmed that the heat pretreatment has a great influence on the properties of the formed emulsion gels.[12,14]

The main objective of this work was undertaken to investigate and compare the mechanical and microstructural properties of cold-set emulsion gels by GDL, CaCl$_2$, and MTGase from SPI-stabilized emulsions. The SPI emulsions were prepared using microfluidization emulsification. The influence of thermal treatments before and/or after emulsification was evaluated. The microstructures of the emulsions or emulsion gels were characterized using confocal laser scanning microscopy (CLSM).

■ MATERIALS AND METHODS

Materials. Defatted soybean meal, obtained by flash desolventization and then drying at 60 °C under vacuum, was provided by Shandong Yuwang Industrial and Commercial Co. Ltd. (China). L-Glutamic acid γ-monohydroxamate and N$_α$-CBZ-GLN-GLY were purchased from Sigma Chemical Co. (St. Louis, MO). CaCl$_2$, GDL, and Rhodamine B (analytical grade) were purchased from Beijing DINGGUO Biological Technology Co. Ltd. (China). Nile blue was purchased from Shanghai BAOAO Biological Technology Co. Ltd. (China). Commercial MTGase was purchased from TAIXIN YIMIN Fine Chemical Industry Co. Ltd. (Jiangsu province, China). The activity of the enzyme product was 200 units/g as determined by a colorimetric procedure using N$_α$-CBZ-GLN-GLY as the substrate and L-glutamic acid γ-monohydroxamate as the standard.[18] The stock enzyme solution was prepared on the basis of our previous work.[19] Soy oil was purchased from the local supermarket (Guangzhou, China). All other chemicals were of analytical grade.

Preparation of SPI. SPI was prepared from defatted soybean meal. In brief, the soybean meal (100 g) was dispersed in distilled water at a solid/solvent ratio of 1:15 (w/v), and the pH of the dispersion was adjusted to 8.0 with 2.0 M NaOH. The dispersion was stirred at room temperature for 2 h and then centrifuged at 8000g for 30 min at 10 °C. The resultant supernatant was adjusted to pH 4.8 with 2.0 M HCl, stirred for 1 h, and then further subjected to centrifugation at 5000g for 20 min (at 10 °C). The pellet was redispersed in distilled water, and the pH was adjusted to 7.5 with 2.0 M NaOH. After dialysis against distilled water for 24 h, the protein dispersion was freeze-dried to produce SPI. The protein content (N × 5.85) of the obtained SPI was 85.6 wt % as determined by using the micro-Kjeldahl method.

SPI Emulsion Preparation. SPI was dispersed in distilled water with 0.04% (w/v) sodium azide and stirred at room temperature for 2 h.

Two SPI dispersions were adjusted to pH 7.0 with 0.2 M NaOH and kept overnight at 4 °C. One SPI dispersion (unheated; control) was directly subjected to preparation of the emulsion. Another SPI dispersion (heated) was heated at 90 °C for 5 min (after the temperature of the dispersion reached about 80 °C) in a water bath, before emulsification. When the SPI emulsions were prepared, the protein concentration in continuous phase was always 6% (w/v) and the oil volume fraction (∅) 0.2.

The unheated and heated SPI dispersions were mixed with soy oil using a high-speed blender operating at 10000 rpm for 3 min (Ultra-Turrax, IKA-Labortechnik, Staufen, Germany) to obtain coarse emulsions. The coarse emulsions were further homogenized at 40 MPa three times using a microfluidizer (Microfluidics Co., USA), to produce two emulsions (denoted emulsions I and II from unheated and heated SPI dispersions, respectively). Emulsions III and IV corresponded to emulsions I and II, which were further heated at 90 °C for 5 min and then cooled immediately in an ice bath, respectively. All of the obtained emulsions were stored at 4 °C before use.

Evaluation of Emulsion Characteristics. *Droplet Size Analysis.* Dynamic light scattering (DLS) using a Zetasizer Nano ZS (Malvern Instruments Ltd., Malvern, Worcestershire, U.K.) equipped with a 4 mW helium/neon laser at a wavelength output of 633 nm was used to record the mean hydrodynamic diameter (z-average diameter) of emulsion samples. The relative refractive index of the emulsion was taken as 1.095, that is, the ratio of the refractive index of soy oil (1.456) to that of the continuous phase (1.33).

Zeta (ζ) Potential Determination. The emulsions were diluted to around 0.005% (v/v) droplet concentration using appropriate background buffer solution and analyzed for ζ-potential measurements by a laser Doppler velocimetry and phase analysis light scattering (M3-PALS) technique using a Malvern Zetasizer Nano ZS (ZEN 3600) instrument (Malvern Instruments Ltd.), in connection with a multipurpose autotitrator (model MPT-2, Malvern Instruments Ltd.). One milliliter of each diluted sample was put in an electrophoresis cell (model DTS 1060C, Malvern Instruments Ltd.). The temperature of the cell was maintained at 25 °C.

Preparation of Emulsion Gels. The emulsion gels were formed using GDL, CaCl$_2$, and MTGase, as the coagulants, in sealed glass cylinders (25 × 25 cm). The formation of emulsion gels induced by various coagulants at various coagulant levels was evaluation by visual observation (based on emulsion I). From the preliminary experiments, optimal conditions (e.g., an optimal coagulant level) for producing the emulsion gels with various coagulants were obtained, on which various emulsion gels were prepared from various emulsions (I−IV).

(1) GDL-Induced Gels. The emulsions were mixed with GDL stock solution (25%, w/v) up to a concentration of 0.2% (w/v); the obtained mixtures were then heat-treated in a water bath with a temperature of 70 °C for 30 min and cooled in ice bath to room temperature. The heat pretreatment not only resulted in a decrease in pH, due to disruption of GDL into gluconic acid, but also accelerated the interactions between protein-coated oil droplets.

(2) CaCl$_2$-Induced Gels. The emulsions were mixed with CaCl$_2$ stock solution up to a concentration of 8 mmol; the mixtures were also heat-treated at 70 °C for 30 min and then cooled to room temperature. In this case, the main role of heat pretreatment was to strengthen interactions between Ca^{2+} and effective sites on the proteins.

(3) MTGase-Induced Gels. The emulsions were mixed with MTGase stock solution (see section 2.1) up to an enzyme concentration of 50 units/g of protein; the mixtures were incubated at 37 °C for 20 h and then cooled in an ice bath to room temperature. All of the obtained gel samples were stored at 4 °C for 20 h, prior to the analyses.

Evaluation of Gel Characteristics. *Mechanical Properties.* The large deformation rheology was applied to evaluate the mechanical properties of emulsion gel samples according to the method of Renkema

Table 1. pH, Zeta Potential, and Mean Droplet Size of Microfluidized SPI Emulsions Prepared by Thermal Treatments before and/or after Emulsification. [a]

parameter	emulsions prepared at various conditions[b]			
	I	II	III	IV
pH	7.23	7.18	7.15	6.88
zeta potential (mV)	−53.1 ± 3.8 a	−44.2 ± 1.6 b	−42.7 ± 2.5 b	−37.7 ± 2.9 c
mean droplet size (nm)	507.8 ± 2.1 a	477.6 ± 3.2 b	468.7 ± 1.6 c	451.1 ± 2.7 d

[a] Data are the means and standard deviations of two determinations. Different letters (a−d) indicate significant difference at the $p < 0.05$ level among different emulsions. [b] I, SPI emulsion (control) prepared from native SPI solution; II, SPI emulsion prepared from heated SPI solution; III, heated SPI emulsion I; IV, heated SPI emulsion II. The heating treatment was carried out at 90 °C for 5 min.

and others[20] and Broersen and others,[21] with a few modifications. The emulsion gels formed in sealed glass cylinders (25 × 25 cm) were tested for fracture using a TA.TX2 texture analyzer (Stable Micro System, Surrey, U.K.) and a measuring probe with a diameter of 5.0 mm. The tests operating at a constant probe speed of 1.0 mm/s were performed, until the threshold force exceeded 1.0 g. The probe penetrated the gels to a deformation of 50% sample height. The measurements were performed at room temperature in duplicate, and mean values with their standard deviations for fracture stress and strain were calculated.

The relative deformation at a certain stage is expressed as a true or Hencky strain ε_h, defined as

$$\varepsilon_h = \ln[h(t)/h_0] \tag{1}$$

where h_0 is the original height of the test gel and $h(t)$ the height after a certain deformation time t. For puncture, the Hencky strain is negative, but it will be expressed as a positive figure.

The average stress in the test sample during deformation at time t, $\sigma(t)$ (Pa), is given by

$$\sigma(t) = F(t)/A(t) \tag{2}$$

where $F(t)$ is the force per unit of area $A(t)$. Assuming that the volume of the test gel (under the probe) does not change during puncture and that its shape remains cylindrical, the cross-section area of the test gel at time t is

$$A(t) = h_0 \times A_0/h(t) \tag{3}$$

From the stress−strain curves, Young's modulus E (Pa), or relative change in stress as a function of change in strain, was calculated from the resulting stress−strain curves by the definition

$$E = [d\sigma/d\varepsilon]_{\varepsilon \to 0} \tag{4}$$

WHC Determination. After the mechanical analysis, the emulsion gel samples (5 g each) were subjected to WHC measurement according to the method of Wu et al.,[22] with a slight modification. The gel samples were transferred to 50 mL centrifuge tubes and centrifuged at 8000*g* for 30 min at 4 °C. Tubes were inverted to drain, and the residue water was carefully removed using dry filter paper. The tubes with the gel samples before and after the centrifugation were accurately weighted. WHC (%) was defined as the ratio of the water weight in the pellet to the water weight in the original gel multiplied by 100.

CLSM. The microstructure of the SPI emulsions and emulsion gels was determined in a confocal laser scanning microscope (Leica TCS SP5, Heidelberg, Germany), using Rhodamine B and Nile blue as fluorescence dyes for the protein and oil phases, with excitation wavelengths at 488 and 633 nm, respectively.[23,24] Both stock dye solutions (1.0%, w/v) were mixed with the emulsions up to concentrations of about 0.05% (w/v), before gel formation. The emulsion gels containing the dyes (with a total amount of 80 μL) were prepared in concave confocal microscope slides (Sail; Sailing Medical-Lab Industries

Co. Ltd., Suzhou, China), covered with glycerol-coated coverslips (which were further sealed with tin foil), according to the same processing as mentioned above. Finally, the CLSM images were obtained with a 100× magnification lens.

All of the fluorescence images were obtained at the same time using both dyes Rhodamine B (for protein) and Nile blue (for oil phase or particle). The overlay images can permit location of the two dyes with respect to each other. The oil phases or particles dyed with the Nile blue are usually green, whereas the proteins dyed with the Rhodamine B are red. Factually, most of the protein-coated oil droplets would be predominantly yellow in appearance of the overlay image (green + red → yellow).

Statistical Analysis. An analysis of variance (ANOVA) of the data was performed, and a least significant difference (LSD) with a confidence interval of 95% was used to compare the means.

■ RESULTS AND DISCUSSION

Emulsion Characteristics. The pH, zeta potential (ζ), and mean droplet size (z-average) of four SPI emulsions (I−IV), applied in this work, are summarized in Table 1. The pH of emulsion I (control) was 7.23, slightly higher than those (pH 7.15−7.18) of emulsions II and III. The decreases in pH by the heating before or after emulsification can be attributed to deamidation of ionized groups (e.g., ε-amide) in soy proteins.[25] The extent of deamidation was most distinct for emulsion IV (pH 6.88; Table 1), where combined heating treatments before and after emulsification were applied. The ζ potential of the emulsions also progressively decreased in the same order as the pH. Especially in emulsion IV, the ζ potential (−37.7 mV) was considerably lower than that (−53.1 mV) of the control (Table 1). This phenomenon is partially due to decreased pH in the system by heating.

The droplet size distribution of the emulsions was measured using a DLS technique. All of the emulsions exhibited a mono-modal droplet size distribution with a relatively symmetrical peak (data not shown). The narrow size distribution was further confirmed by CLSM (Figure 1), by which it was observed that all of the oil droplets with similar sizes, dyed with the Nile blue (green color), were evenly dispersed in the emulsions. The mean droplet diameter of all the emulsions was in the same range of 450−500 nm, although there were slight but significant changes in mean droplet diameter among the various emulsions (Table 1). In general, the heating treatments before and/or after emulsification led to decreases in mean droplet diameter. The decreases by heating before the emulsification could be well understood, because the heating might lead to protein unfolding and subsequent exposure of hydrophobic domains initially buried within the soy protein molecules, thus resulting in the

improvement of their emulsifying properties. By comparison, the decreases in mean droplet diameter by heating after emulsification seem to be unreasonable, because it is generally recognized that the heating usually results in flocculation of oil droplets in protein-stabilized emulsions.[26] However, it should be noted that the emulsions in the present work were obtained by microfluidization emulsification with much higher energy input than other conventional emulsification techniques. Dynamic high-pressure shearing during microfluidization treatment might lead to changes in ternary and/or quaternary conformations of the proteins.[27] In the present case, these unfolded soy proteins would interact with the proteins coated on the surfaces of the oil droplets, possibly through hydrophobic interactions, and as a consequence, some kind of aggregated oil droplets might be present in the emulsion systems. This phenomenon is evidenced by the CLSM observation that in the microfluidized emulsions, protein-coated oil droplets were irregular in morphology and even present in the form of droplet clusters (Figure 1). Thus, decreases in mean droplet diameter by heating after emulsification could be associated with enhanced intramolecular
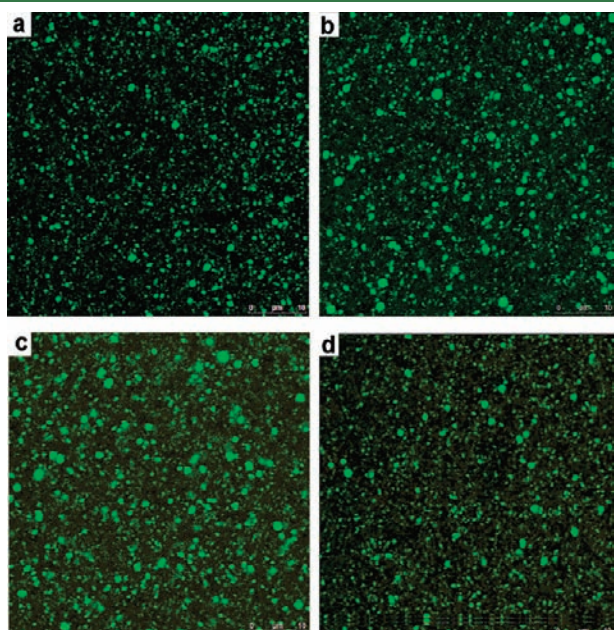
Figure 1. CLSM images of four kinds of SPI emulsions: a, emulsion I; b, emulsion II; c, emulsion III; d, emulsion IV. Emulsions I–IV refer to footnote *b* of Table 1. The images were obtained with the fluorescent dye Nile blue.

hydrophobic interactions of unfolded soy proteins that might lead to formation of more compact conformations for the proteins coated on the surfaces of oil droplets.

Mechanical Properties. Mechanical properties of formed SPI emulsion gels were determined by penetration analysis. From stress–strain curves, fracture stress (σ_f) and strain (ε_f) and Young's modulus (E) of various SPI emulsion gels were obtained, as summarized in Table 2. The large deformation mechanical properties could reflect information about gel network structure.[20] Gels that fracture at low strain values usually have networks composed of relatively thin strands and small, homogeneous pores, whereas gels that fracture at high strain values have thicker strands and relatively large, inhomogeneous pores.[28]

The σ_f and ε_f considerably varied among the formed gels with various coagulants from various emulsions (Table 2), indicating differences in gel network structure. The application of GDL and CaCl$_2$ as the coagulants could result in gel formation of all test emulsions (I–IV). In these casthees, the σ_f values (24.6–30.8 and 16.0–22.5 kPa) of emulsion III and IV gels were considerably higher than those (7.5–9.4 and 4.0–8.6 kPa) of emulsion I and II gels (Table 2). In contrast, the application of MTGase as the coagulant led only to gel formation for emulsions I and II and did not form gel for emulsions III and IV. Apparently, heating after emulsification altered the structure of the proteins at the oil/water interface and considerably decreased the effective catalytic sites for MTGase. As a consequence, the cross-links between protein-coated oil droplets were not enough for gel formation of the emulsions. In our previous work about MTGase-induced tofu from soy milk, it was similarly found that the gel hardness of tofu from soy milk heat-pretreated at 95 °C was remarkably lower than that from soy milk heat-pretreated at 75 °C.[28] In this work, this has also been attributed to the decrease in the catalytic efficiency of covalent cross-linking by MTGase, due to severe aggregation of soy proteins in soy milk. However, the mechanical strength of MTGase-induced emulsion I or II gels was much greater than that of GDL or CaCl$_2$-induced emulsion III and IV gels. For example, the σ_f of the former emulsion I gel was approximately 2.0 and 1.4 times that of GDL- and CaCl$_2$-induced emulsion III gels, respectively (Table 2). The data suggest that the preparation of SPI emulsions is of vital importance for the production of the related emulsion gels.

In the GDL- and CaCl$_2$-induced gels, the highest σ_f values were observed for emulsion III (Table 2), when the heating was carried out after emulsification. Heating before emulsification significantly decreased the strength of the corresponding gels, irrespective of heating after emulsification (with an exception for CaCl$_2$-induced emulsion I and II gels, when the heating led to

Table 2. Fracture Strain (ε_f) and Stress (σ_f) and Young's Modulus (E) of SPI Emulsion Gels, Induced by CaCl$_2$, GDL, and MTGase, Respectively[a]

emulsion	CaCl$_2$-induced gels			GDL-induced gels			MTGase-induced gels		
	σ_f (kPa)	ε_f	E (kPa)	σ_f (kPa)	ε_f	E (kPa)	σ_f (kPa)	ε_f	E (kPa)
I	9.4 ± 0.5 b,f	0.401 ± 0.009 a,f	74.6 ± 4.0 a,g	7.5 ± 0.1 c,f	0.398 ± 0.009 a,e	74.2 ± 4.0 a,f	45.0 ± 2.4 a,d	0.383 ± 0.005 b,d	78.6 ± 7.8 a,d
II	8.6 ± 0.9 b,f	0.383 ± 0.003 b,g	104.5 ± 6.0 a,f	4.0 ± 0.5 c,g	0.399 ± 0.008 a,e	32.2 ± 3.0 c,g	20.0 ± 1.2 a,e	0.302 ± 0.032 c,f	45.0 ± 9.0 b,e
III	30.8 ± 0.4 a,d	0.444 ± 0.007 a,d,	393.6 ± 3.3 a,d	24.6 ± 3.8 b,d	0.373 ± 0.052 b,e	290.1 ± 3.2 b,d	—	—	—
IV	22.5 ± 0.5 a,e	0.422 ± 0.007 b,e,	272.6 ± 7.3 a,e	16.0 ± 2.6 b,e	0.445 ± 0.013 a,d,	270.8 ± 7.3 a,e	—	—	—

[a] All of the gels were formed at optimal conditions. Data are the mean and standard deviation of duplicate measurements. Different letters (a–c) indicate significant difference at the $p < 0.05$ level among SPI emulsion gels, induced by various coagulants (for a given SPI emulsion). Different letters (d–g) indicate significant difference at $p < 0.05$ among the emulsion gels, prepared from various SPI emulsions (induced by a specific coagulant). The character (—) represents no gel formation. Emulsions I–IV refer to footnote *b* of Table 1.

slight but insignificant decreases in σ_f). These phenomena suggest that the formation of thermal protein aggregates before emulsification is not favorable for gel formation, whereas heating after emulsification could greatly improve gel formation. In contrast to this, the coagulant MTGase only gelled emulsions I and II (Table 2). This phenomenon indicated that heating before or after emulsification was unfavorable for the emulsion gel network formation by MTGase. In the MTGase-induced gels, the σ_f (45 kPa) of the emulsion I gel was >2 times that (20 kPa) of the emulsion II gel (Table 2). This further confirmed the influence of heating on the gel network formation.

Heating before and/or after emulsification also led to significant changes in ε_f of the gels, depending on the type of emulsions and applied coagulants (Table 2). In the CaCl$_2$ case, emulsion III and IV gels had significantly higher ε_f than those from emulsions I and II, indicating that the heating after emulsification increased the deformation capacity of the gels. In other words, heating after emulsification led to the formation of emulsion gels with thicker strands and more large and inhomogenous pores.[29] However, the gels formed from heated protein solutions fractured at significantly ($p < 0.05$) less strain values than those from unheated protein solutions (Table 2), indicating differences in gel network structure. Nevertheless, in the GDL case, a significantly higher ε_f was observed only for the emulsion IV gel (relative to other emulsion gels), indicating that the network structure of the emulsion IV gel was different from that of other GDL-induced gels. In contrast, the ε_f of MTGase-induced gels was significantly ($p < 0.05$) lower than that of other gels (from emulsion I or II) (Table 2), suggesting that the network structure of MTGase-induced gels was composed of much less thick strands and more homogeneous pores.

The Young's modulus (E) data of the emulsion gels, determined from the initial slope of the stress−strain curve, are also included in Table 2. In the cases using CaCl$_2$ and GDL as the coagulants, E shows the same trends as the σ_f, indicating that the gel stiffness of CaCl$_2$- and GDL-induced emulsion gels was consistent with the gel strength. The CaCl$_2$- and GDL-induced emulsion III and IV gels exhibited much higher E values than emulsion I and II gels, indicating that heating after emulsification greatly increased gel stiffness. In these cases, the E value was about 8−10 times the σ_f value. In contrast, the E/σ_f ratio of the MTGase-induced gels was much less (only about 1.7−2.2-fold) (Table 2), although these gels fractured at much higher threshold force (relative to other types of gels). The E data were obtained at much less strain ($\varepsilon \approx 0.05-0.1$), whereas the σ_f was determined at strain of 0.3−0.4. Thus, the difference in the E/σ_f ratio reflects that the gel formation mechanism by MTGase was distinctly different from that by CaCl$_2$ and GDL.

WHC. The WHC data of the formed emulsion gels are shown in Table 3. As expected, various formed gels exhibited considerable differences in WHC. Although the MTGase-induced emulsion I gel had much higher mechanical strength than GDL- and CaCl$_2$-induced emulsion gels, the WHC (53.5%) of the former was considerably lower than that (71.1 and 82.7%) of the latter two gels, respectively. The heating before emulsification resulted in a slight decrease in WHC of GDL- and CaCl$_2$-induced gels, but significantly increased the WHC of the MTGase emulsion gel (Table 3). Heating after emulsification, on the contrary, significantly increased the WHC of the GDL and CaCl$_2$ emulsion gels. Together with the σ_f data (Table 3), it could be considered that the improvements of the WHC in these two cases was due to strength enhancement of the gel structure by the heating,

Table 3. Water-Holding Capacity (WHC; Percent) of SPI Emulsion Gels, Induced by GDL, CaCl$_2$, and MTGase, Respectively[a]

| emulsion	GDL-induced gels	CaCl$_2$-induced gels	MTGase-induced gels
I	71.1 ± 2.0 b,e	82.7 ± 3.5 a,d	53.5 ± 1.4 c,e
II	67.1 ± 1.8 b,e	77.9 ± 1.9 a,e	58.8 ± 1.1 b,d
III	78.8 ± 1.2 b,d	87.3 ± 2.5 a,d	−
IV	79.8 ± 1.5 a,d	82.8 ± 2.2 a,de	−

[a] Data are the mean and standard deviations of duplicate measurements. Different letters (a−c) indicate significant difference at the $p < 0.05$ level among SPI emulsion gels, induced by various coagulants (for a given SPI emulsion). Different letters (d−g) indicate significant difference at $p < 0.05$ among the emulsion gels, prepared from various SPI emulsions (induced by a specific coagulant). The character (−) represents no gel formation. Emulsions I−IV refer to footnote b of Table 1.

possibly through strengthened hydrophobic interactions of the proteins on the oil particle interfaces. Colloidal interactions between droplets resulting from heat-induced unfolding and subsequent aggregation of protein molecules adsorbed at the oil−water interface have been recognized in many previous literature studies of whey protein-stabilized emulsions.[30,31]

The much more decreased WHC for the MTGase-induced gels (relative to the GDL- and CaCl$_2$-induced gels; Table 3) seems to be unreasonable, because the gel network for the former was much stronger, especially based on emulsion I (control). One reasonable explanation is that not only the network but also the charged groups of the proteins in the systems might contribute to the water retention of the emulsion gels. In this case, the considerable decrease in charged groups (e.g., ε-amino groups of Lys residues) by the enzymatically induced cross-linking may partially account for this phenomenon.[32]

Microstructure. The CLSM technique was applied to characterize microstructures of SPI emulsion gels, formed by various coagulants from various emulsions (I−IV). Typical CLSM images of various SPI emulsion gels (or dispersions) are presented in Figure 2. As expected, the microstructures of the formed gels considerably varied with the type of applied coagulant and initial emulsion. In general, filamentous networks were observed for GDL- and MTGase-induced emulsion gels, whereas in the CaCl$_2$ case, the gel network of all the emulsion gels was composed of particulate clusters or clumps of oil droplets (Figure 2). The differences in microstructure are clearly attributed to the differences in gel formation mechanism. In the GDL and MTGase cases, the driving forces to form the gel network seem to be isotropic, and as a result, the formed gels would be homogeneous in gel network. In these cases, there would be a "critical gelation point" at which the state of the system might transform from "sol" to "gel", whereas in the Ca^{2+} case, the driving forces (e.g., Ca^{2+}-bridges between protein-coated oil droplets) to form aggregated oil droplets are usually strong and the process would be fast. As a consequence, the emulsion gel formation is instant, although in this case, the gel strength would be strengthened upon further incubation.

The images of GDL-induced emulsion I and II gels were to a relatively higher extent red than were the emulsion III and IV gels (Figure 2, first row), indicating that in the former cases, the gel network might be predominantly composed of filamentous protein aggregates (yellow color), and the oil droplets (green color) seemed to be largely entrapped within the network, whereas in the latter cases, the network might be mainly

4075

dx.doi.org/10.1021/jf104834m |*J. Agric. Food Chem.* 2011, 59, 4071–4077
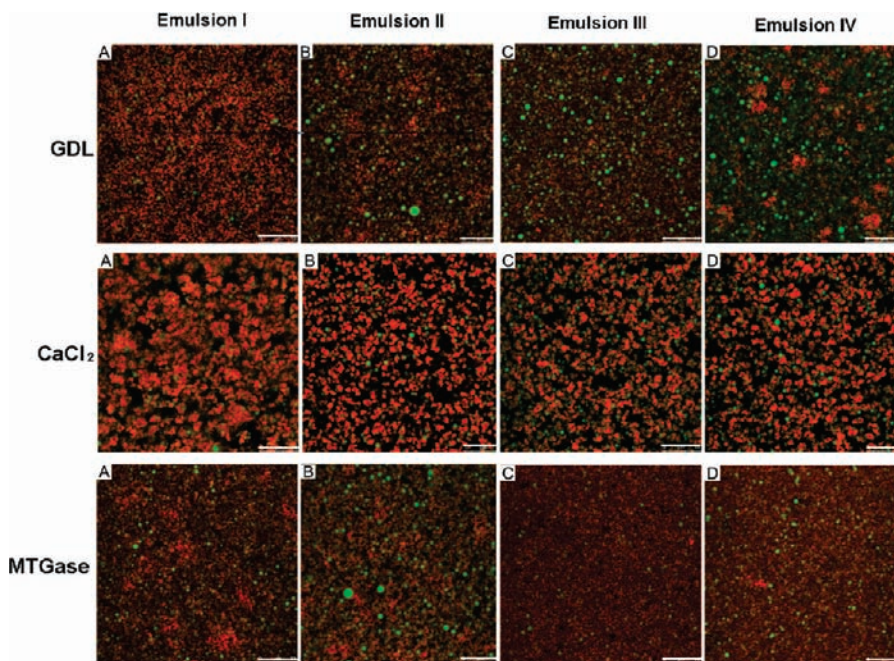
Figure 2. CLSM images of SPI emulsion gels (or dispersions), formed from four SPI emulsions (I−IV) by GDL, CaCl$_2$, and MTGase, respectively. All of the images were obtained with the dyes Rhodamine B (protein) and Nile blue (oil phase), excited at 488 and 633 nm, respectively. Columns A−D correspond to emulsions I−IV, respectively (refer to footnote b of Table 1). The bars indicate 10 μm in length.

composed of both filamentous protein aggregates and protein-coated oil droplets. Although it is well recognized that protein-coated oil droplets can act as "active fillers" in the emulsion gel formation,[2,6,7] their role in the gel network is affected by interactions between the unadsorbed proteins and those coated on the surface of oil droplets. Taking together the fracture data (Table 2), it can be reasonably hypothesized that in the GDL case, heating after the emulsification greatly improved the role of protein-coated oil droplets as a kind of active filler in the emulsion gel formation. Besides the interactions between un-adsorbed proteins and protein-coated oil droplets, the protein−protein interactions of unadsorbed proteins in the systems also greatly affected the network strength of GDL-induced emulsion gels. The combined heating before and after emulsification resulted in the distinct occurrence of the clump-like aggregates (Figure 2, first row, D). This phenomenon is well in agreement with the lower gel strength of the emulsion IV gel (relative to the emulsion III gel; Table 2), clearly indicating that severe protein aggregation greatly impaired the gel network.

In the CaCl$_2$ case, it can be also observed that the obtained images of the emulsion I and II gels were to a relatively higher extent red than were the emulsion III and IV gels (Figure 2, second row), indicating that heating after the emulsification improved the role of protein-coated oil droplets in the gel network formation. In fact, this is consistent with many previous observations in the heat-induced gelation case that the protein-coated oil droplets act as a kind of active filler in the emulsion gel formation.[2,6,7] In the present work, the heating after the emulsi-fication might increase the interactions between unadsorbed proteins and protein-coated oil droplets. In the emulsion I gel, the aggregated protein-coated oil droplets were present even in the form of clusters or clumps (Figure 2, second row, A), which is clearly unfavorable for gel network formation. These phenomena are basically consistent with the σ_f data (Table 2), indicating that

in the CaCl$_2$ case, the higher gel strength of emulsion III or IV gels was closely related to that of the more protein-coated oil droplets involved in the gel network formation than that of emulsion I or II gels.

In contrast to the predominantly red appearance of the emulsion III or IV dispersions (where no gelation occurred), the images of the MTGase-induced emulsion I and II gels exhibited a distinct yellow appearance (Figure 2, third row). This phenomenon of yellow appearance is indirect evidence showing that the gel network in MTGase-induced emulsion gels involved both the unadsorbed proteins (red) and protein-coated oil droplets (green). By comparison, it can be observed that in the emulsion I gel, more protein-coated oil droplets were entrapped within the gel network, and even involved in the gel network formation, than in the emulsion II gel (Figure 2, third row, A, B). In the latter gel, there were also some clefts observed (Figure 2, third row, B). The difference in microstructure is in accordance with the fracture data (Table 2), indicating that heating after emulsification greatly impaired the MTGase-induced emulsion gel formation. The underlying mechanism is clearly due to decreased cross-linking efficiency among various proteins or protein-coated oil droplets alone, or one another. In general, the network structure of MTGase-induced emulsion I or II gels was composed of much more homogeneous and thinner strands and smaller pores than GDL- or CaCl$_2$-induced gels (Figure 2), which is basically in agreement with the fracture data (Table 2), confirming close relationships between their mechanical proper-ties and microstructure.

In conclusion, the properties and microstructures of SPI emulsion gels induced by various coagulants considerably varied. The properties and microstructures were also highly affected by heating treatments before and/or after emulsification. In the GDL- and CaCl$_2$-induced cases, the emulsion gels could be formed, irrespective of the type of the emulsions, but the gel

strength of the emulsion gels from the heated emulsions was much higher than those from unheated ones. In the MTGase case, emulsion gel formation was observed only from unheated emulsions. Nevertheless, the gel strength of MTGase-induced emulsion gels was significantly much higher than the GDL and CaCl$_2$ gels. The WHC of MTGase-induced emulsion gels was much lower than that of other gels. The GDL- or MTGase-induced emulsion gels exhibited filamentous gel networks, whereas the CaCl$_2$-induced gel was mainly composed of particulate protein-coated oil droplets. The results indicated close relationships between physicochemical properties and microstructures of SPI emulsion gels. These results would be of vital importance for extending the present knowledge about the preparation and properties of emulsion gels from soy protein-stabilized emulsions.

■ AUTHOR INFORMATION

Corresponding Author
*Phone: (086)20-87111707. Fax: (086)20-87114263. E-mail: chtang@scut.edu.cn.

■ REFERENCES

(1) Dickinson, E.; Yamanoto, Y. Rheology of milk protein gels and protein-stabilized emulsion gels cross-linked with transglutaminase. *J. Agric. Food Chem.* **1996**, *44*, 1371–1377.

(2) Chen, J.; Dickinson, E. Viscoelastic properties of protein-stabilized emulsions: effect of protein-surfactant interactions. *J. Agric. Food Chem.* **1998**, *46*, 91–97.

(3) Sok Line, V. L.; Remondetto, G. E.; Subirade, M. Cold gelation of β-lactoglobulin oil-in-water emulsions. *Food Hydrocolloids* **2005**, *19*, 269–278.

(4) Liang, L.; Sok Line, C. L.; Remondetto, G. E.; Subirade, M. In vitro release of α-tocopherol from emulsion-loaded β-lactoglobulin gels. *Int. Dairy J.* **2010**, *20*, 176–181.

(5) Boutin, C.; Giroux, H. J.; Paquin, P.; Britten, M. Characterization and acid-induced gelation of butter oil emulsions produced from heated whey protein dispersions. *Int. Dairy J.* **2007**, *17*, 696–703.

(6) Chen, J.; Dickinson, E. Viscoelastic properties of heat-set whey protein emulsion gels. *J. Texture Stud.* **1998**, *29*, 285–304.

(7) Chen, J.; Dickinson, E. Effect of surface character of filler particles on rheology of heat-set whey protein emulsion gels. *Colloid Surface B* **1999**, *12*, 373–381.

(8) Chen, J.; Dickinson, E.; Langton, M.; Hermansson, A.-M. Mechanical properties and microstructure of heat-set whey protein emulsion gels: effect of emulsifiers. *LWT* **2000**, *33*, 299–307.

(9) Dickinson, E.; Chen, J. Heat-set whey protein emulsion gels: role of active and inactive filler particles. *J. Dispersion Sci. Technol.* **1999**, *20*, 197–213.

(10) Dickinson, E.; Hong, S. T.; Yamanoto, Y. Rheology of heat-set emulsion gels containing beta-lactoglobulin and small-molecule surfactants. *Neth. Milk Dairy J.* **1996**, *50*, 199–207.

(11) Kerstens, S.; Murray, B. S.; Dickinson, E. Confocal microscopy of heat-induced aggregation and gelation of β-lactoglobulin in presence of non-ionic surfactant. *Food Hydrocolloids* **2005**, *19*, 625–633.

(12) Rosa, P.; Sala, G.; van Vliet, T.; van de Velde, F. Cold gelation of whey protein emulsions. *J. Texture Stud.* **2006**, *37*, 516–537.

(13) Sala, G.; van Aken, G. A.; Stuart, M. A. C.; van de Velde, F. Effect of droplet-matrix interactions on large deformation properties of emulsion-filled gels. *Texture Stud.* **2007**, *38*, 511–535.

(14) Ye, A.; Taylor, S. Characterization of cold-set gels produced from heated emulsions stabilized by whey protein. *Int. Dairy J.* **2009**, *19*, 721–727.

(15) Kim, K.-H.; Renkema, J. M. S.; van Vliet, T. Rheological properties of soybean protein isoalte gels containing emulsion droplets. *Food Hydrocolloids* **2001**, *15*, 295–302.

(16) Lee, H. A.; Choi, S. J.; Moon, T. W. Characteristics of sodium caseinate- and soy protein isolate-stabilized emulsion-gels formed by microbial transglutaminase. *J. Food Sci.* **2006**, *71*, C352–C357.

(17) Gu, X.; Campbell, L. J.; Euston, S. R. Effects of different oils on the properties of soy protein isolate emulsions and gels. *Food Res. Int.* **2009**, *42*, 925–932.

(18) Folk, J. E.; Cole, P. W. Structure requirements of specific substrates for guinea pig liver transglutaminase. *J. Biol. Chem.* **1966**, *240*, 2591–2960.

(19) Tang, C. H.; Sun, X.; Ma, C. Y. Transglutaminase-induced cross-linking of vicilin-rich kidney protein isolate: Influence on the functional properties and *in vitro* digestibility. *Food Res. Int.* **2008**, *41*, 941–947.

(20) Renkema, J. M. S.; Knabben, J. H. M.; van Vliet, T. Gel formation of β-conglycinin and glycinin and their mixtures. *Food Hydrocolloids* **2001**, *15*, 407–414.

(21) Broersen, K.; van Teeffelen, A. M. M.; Vries, A.; Voragen, A. G. J.; Hamer, R. J.; de Jongh, H. H. J. Do sulfhydryl groups affect aggregation and gelation properties of ovalbumin?. *J. Agric. Food Chem.* **2006**, *54*, 5166–5174.

(22) Wu, M.; Xiong, Y.; Chen, J.; Tang, X.; Zhou, G. Rheological and microstructural properties of porcine myofibrillar protein−lipid emulsion composite gels. *J. Food Sci.* **2009**, *74*, E207–E217.

(23) Kerstens, S.; Mugnier, C.; Murray, B. S.; Dickinson, E. Influence of ionic surfactants on the microstructure of heat-set β-lactoglobulin-stabilized emulsion gels. *Food Biophysics* **2006**, *1*, 133–143.

(24) van den Berg, L.; Rosenberg, Y.; van Boekel, M. A. J. S. Microstructural features of composite whey protein/polysaccharide gels characterized at different length scales. *Food Hydrocolloids* **2009**, *23*, 1288–1298.

(25) Metwalli, A. A. M.; van Boekel, M. A. J. S. On the kinetics of heat-induced deamidation and breakdown of caseinate. *Food Chem.* **1998**, *61*, 53–61.

(26) Kiosseoglou, N. D. V. Stability against heat-induced aggregation of emulsions prepared with a dry-heated soy protein isolate−dextran mixture. *Food Hydrocolloids* **2006**, *20*, 787–792.

(27) Jelen, M. I. P. High pressure microfluidization treatment of heat denatured whey proteins for improved functionality. *Innovative Food Sci. Emerging Technol.* **2003**, *4*, 367–376.

(28) Tang, C. H. Effect of thermal pretreatment of raw soymilk on the gel strength and microstructure of tofu induced by microbial transglutaminase. *LWT−Food Sci. Technol.* **2007**, *40*, 1403–1409.

(29) Roff, C. F.; Foegeding, E. A. Dicationic-induced gelation of predenatured whey protein isolate. *Food Hydrocolloids* **1996**, *10*, 193–198.

(30) Demetriades, K.; Coupland, J. N.; McClememnts, D. J. Physicochemical properties of whey protein-stabilized emulsions as affected by heating and ionic strength. *J. Food Sci.* **1997**, *62*, 462–467.

(31) Raikos, V. Effect of heat treatment on milk protein functionality at emulsion interfaces. A review. *Food Hydrocolloids* **2010**, *24*, 259–265.

(32) Jaros, D.; Partschefeld, C.; Henle, T.; Rohm, H. Transglutaminase in dairy products: chemistry, physics, applications. *J. Texture Stud.* **2006**, *37*, 113–155.